Polar $CsPbBr_3$-Based Dion-Jacobson Hybrid for Promising UV Photodetection

Dongying Fu,*[ab] Shichao Wu,[ab] Jianli Xin,[ab] Xinyuan Zhang,[d] Gaoyi Han,[b] Xian-Ming Zhang,*[ac]

a Institute of Crystalline Materials, Institute of Molecular Science, Shanxi University, Taiyuan, Shanxi 030006, China

b Institute of Molecular Science, Shanxi University, Taiyuan, Shanxi 030006, China
c School of Chemistry and Materials Science, Shanxi Normal University, Linfen, Shanxi 041001, China.
d State Key Laboratory of Structural Chemistry, Fujian Institute of Research on the Structure of Matter, Chinese Academy of Sciences, Fuzhou, Fujian, 350002, P.R. China.
**E-mail: dyfu@sxu.edu.cn (D. Fu), xmzhang@sxu.edu.cn (X.-M. Zhang)*

Table of Content

EXPERIMENTAL SECTION

Synthesis. For the preparation of $(2meptH_2)CsPb_2Br_7$ (**1**), stoichiometric $Pb(AC)_2 \cdot 3H_2O$ (3 mmol) were firstly dissolved in the HBr solution (20 mL, 47%). Subsequently, equimolar Cs_2CO_3 (2 mmol) and 2-methyl-1,5-diaminopentane (2 mmol) were added into the solution, which yields light-yellow powder precipitation. After heating to boiling, a clear light yellow solution was obtained. To grow the bulk crystals of $(2meptH_2)CsPb_2Br_7$ (**1**), the synthesized raw materials were purified by successive recrystallization in HBr solutions. In the growth commencement, the clear saturated solution of **1** was filtrated and maintained 2~3 °C above its saturated temperature for 3 hours. The temperature was cooled at a rate of 1 ℃ per day as the growth progressed. Yellow high-quality single bulk crystal has been acquired after several days (Figure 1). The purity of the as-grown crystals were confirmed by powder X-ray diffraction (PXRD, Figure S1)

Measurements. PXRD pattern was implemented using the Rigaku MiniFlex II diffractometer in the 2θ range of 5° to 50°. The Nd:YAG laser (λ = 1064 nm, 5 ns pulse duration, ~1.6 MW peak power, 10 Hz repetition rate) was used to measure the temperature-dependent second harmonic generation (SHG) signals of **1**, with KH_2PO_4 (KDP) as the reference to evaluate the numerical values of the nonlinear optical coefficients. The optical absorption spectrum of **1** was measured using a Perkin-Elmer Spectrometer. A 375 nm laser (ALS, PiL037x) and a frequency-quadrupled 266 laser from Nd:YAG laser (1064 nm, 5 ns pulse) were used for light illumination. Transient photoelectric responses were collected by using a 1 GHz bandwidth oscilloscope (Tektronix, MDO3012). Two symmetric Ag electrodes with a defined gap of 300 μm were painted on the flat side of a well-polished single crystal. The current vs voltage (*I-V*) and photocurrent vs time (*I-t*) with light on or off under a 375 nm laser light and 266 nm UV laser light were measured using a high precision electrometer (Keithley 6517B). The devices were illuminated by monochromatic light (266 and 375 nm). The light intensity was controlled by varying the current. The actual light intensity was measured using a power meter (CEL-NP2000). The time-dependent photocurrent response was recorded by a current meter after switching the illumination. All the electrical measurements were performed under atmosphere and at room temperature.

Single crystal X-ray diffraction measurements of **1** were performed on a Bruker D8 diffractometer with the Mo *Kα* radiation at 293 K, respectively. The structures of which are solved by direct methods and refined by the full-matrix least-squares refinements on F^2 using *SHELX-97*. The detailed crystal structure data are given in Tables S1.

Calculation method. First-principles density function theory (DFT) calculations were carried out with the CASTEP code.[1,2] At room temperature, the orientations of the $[2meptH_2]^{2+}$ cations in **1** exhibit random distribution from the experimental result. During the calculation, a proposed polar structure with all $[2meptH_2]^{2+}$ cations aligned along the same direction were used. The exchange-correlation functional was described by a generalized gradient approximation (GGA) with Perdew-Burke-Ernzerhof functional for solids (PBEsol) scheme.[3] The interactions between the ionic cores and the electrons were described by the norm-conserving pseudopotential.[4] The following orbital electrons were treated as valence electrons: Pb $6d^{10}6s^26p^3$; Br $4s^24p^5$; C $2s^22p^2$; N $2s^22p^3$ and H $1s^1$. The numbers of plane waves included in the basis sets were determined by a cutoff energy 310 eV. To achieve the accurate density of the electronic states, the *k*-space integrations were done with Monkhorst-Pack grids with a 6 × 6 × 3 *k*-point for compound **1**, respectively. The other parameters and convergent criteria were the default values of CASTEP code.

1. M. D. Segall *et al.* First-principles simulation: ideas, illustrations and the CASTEP code. *J. Phys.: Condens. Matter* 14, 2717-2744 (2002).
2. S. J. Clark *et al.* First principles methods using CASTEP. *Zeitschrift Fur Kristallographie* 220, 567-570 (2005).
3. J. P. Perdew *et al.* Restoring the Density-Gradient Expansion for Exchange in Solids and Surfaces. *Phys. Rev. Lett.* 100, 136406 (2008).
4. D. R. Hamann, Schlüter, M. & Chiang, C. Norm-Conserving Pseudopotentials. *Phys. Rev. Lett.* 43, 1494 (1979).

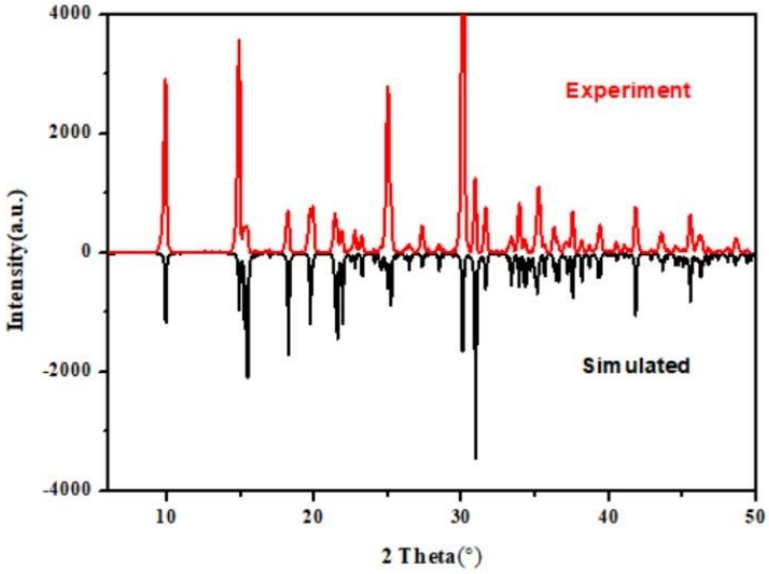

(a)

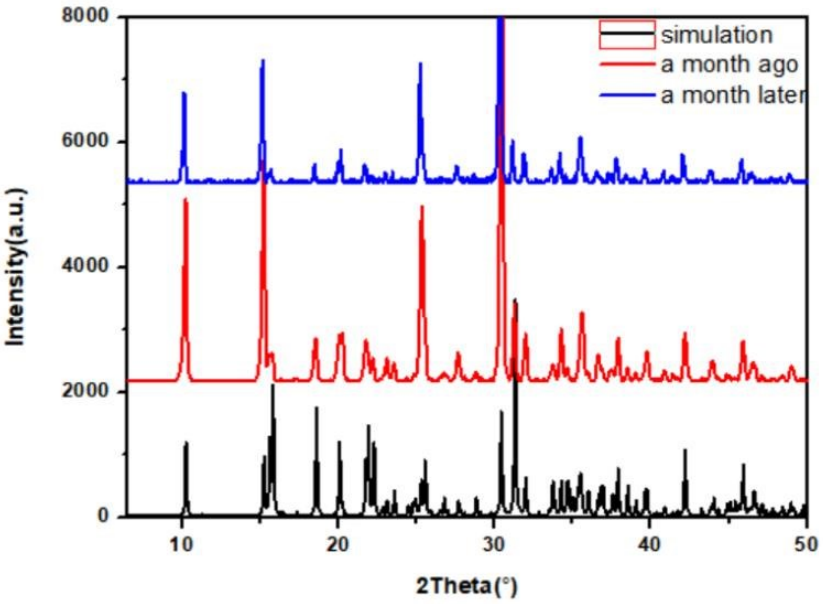

(b)

Figure S1. Experiment and simulated powder X-ray diffraction patterns of **1** at room temperature (a); and structure stability of **1** before and after one month (b).

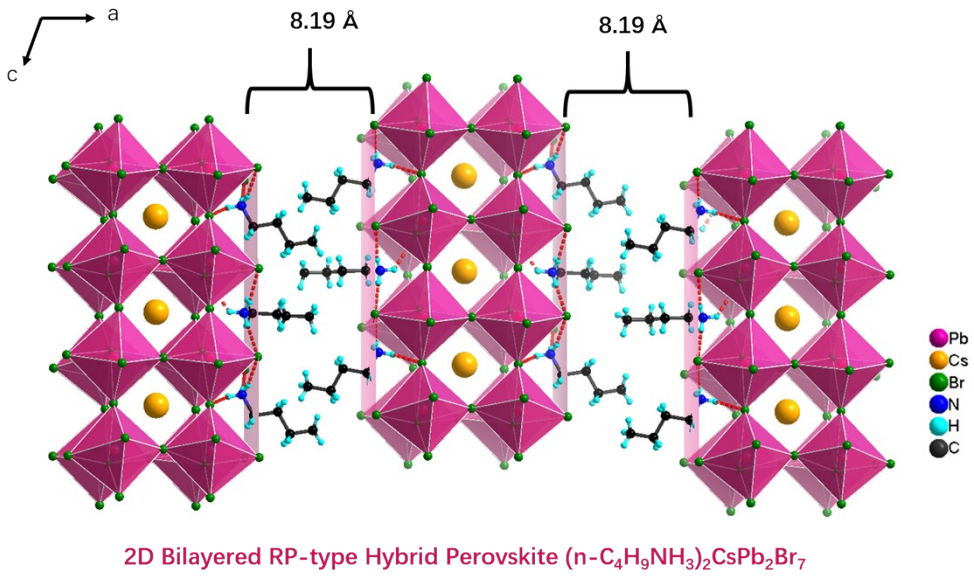

Figure S2. RP-type 2D bilayered (n-$C_4H_9NH_3)_2CsPb_2Br_7$ with interlayer distance of 8.19 Å.

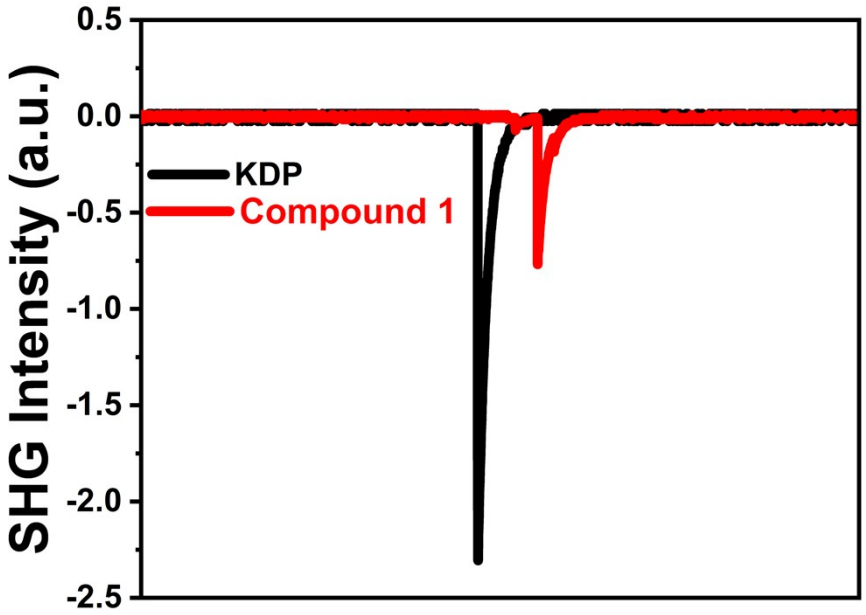

Figure S3. The SHG signals for the KDP standard and the polycrystalline sample of **1** at room temperature.

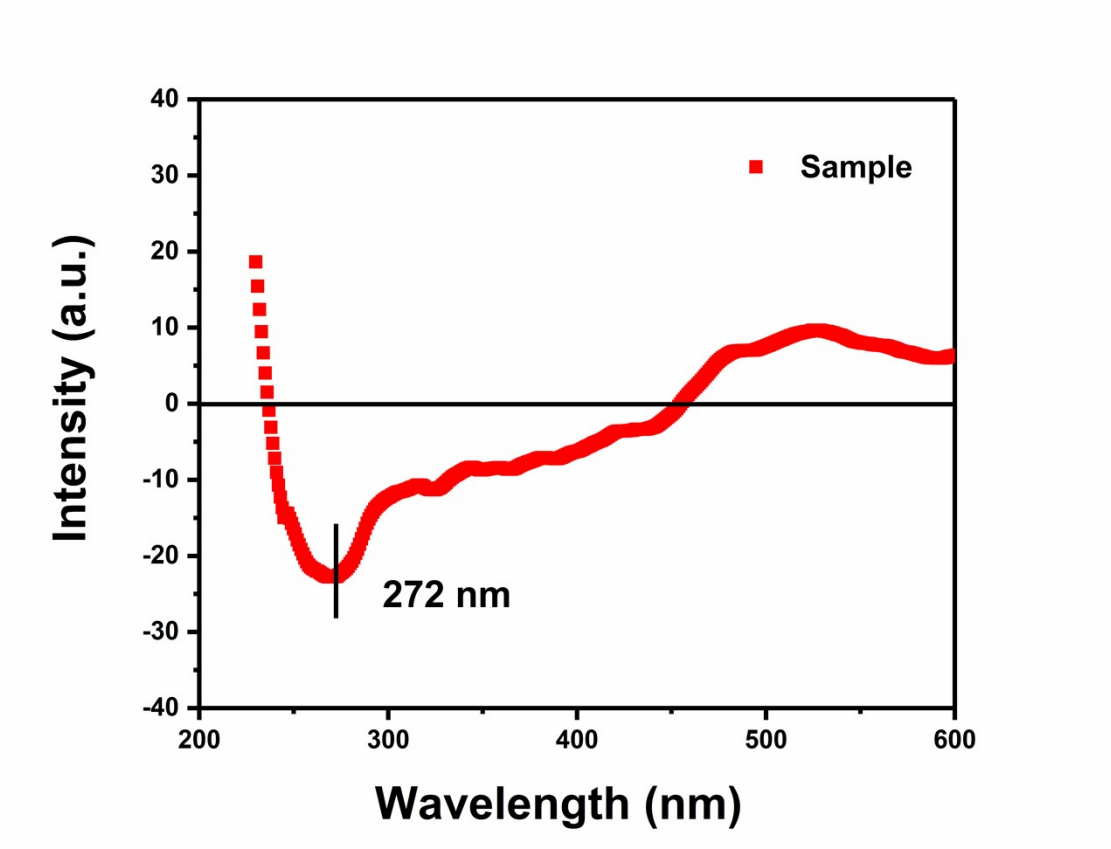

Figure S4. The CD spectra of **1** at room temperature.

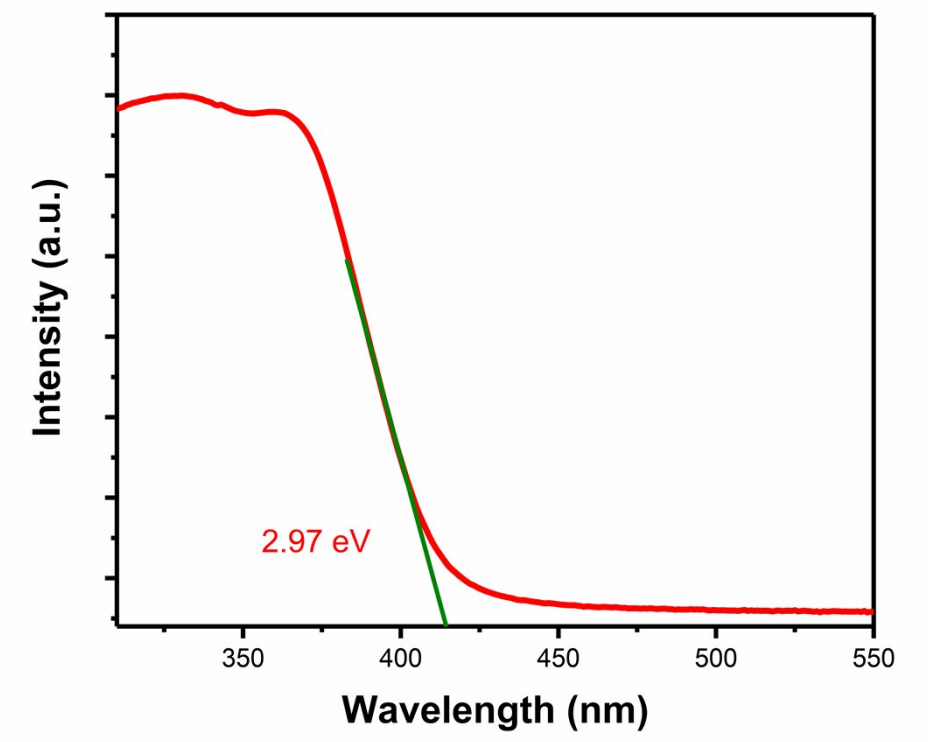

Figure S5. The energy bandgap of **1** deduced from its optical absorption spectrum.

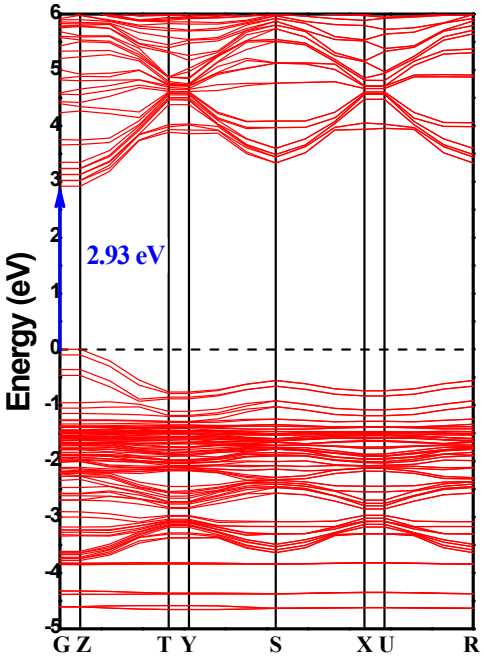

(a)

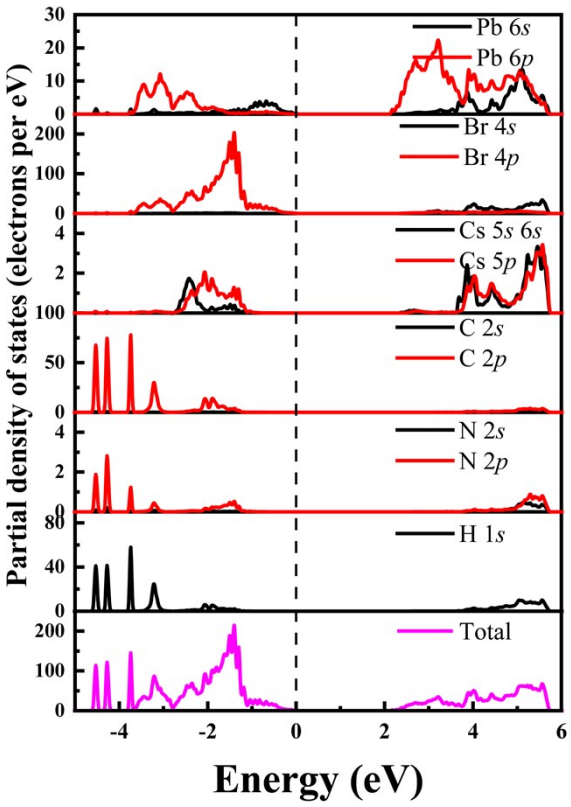

(b)

Figure S6. a) Calculated band structure and b) PDOS spectra of **1**.

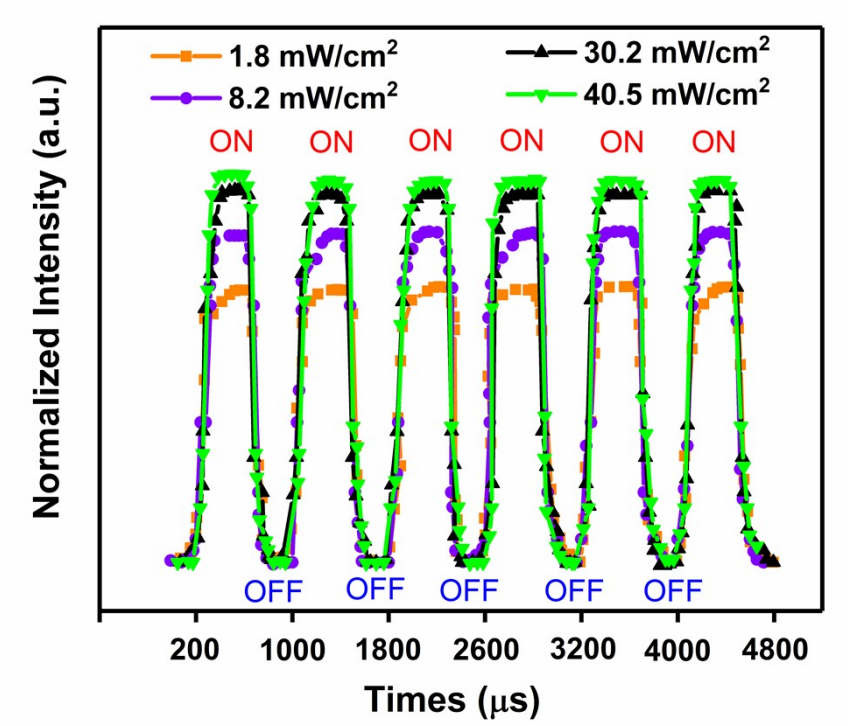

Figure S7. The recyclable switching operation of photocurrent response under 377 nm light illumination.

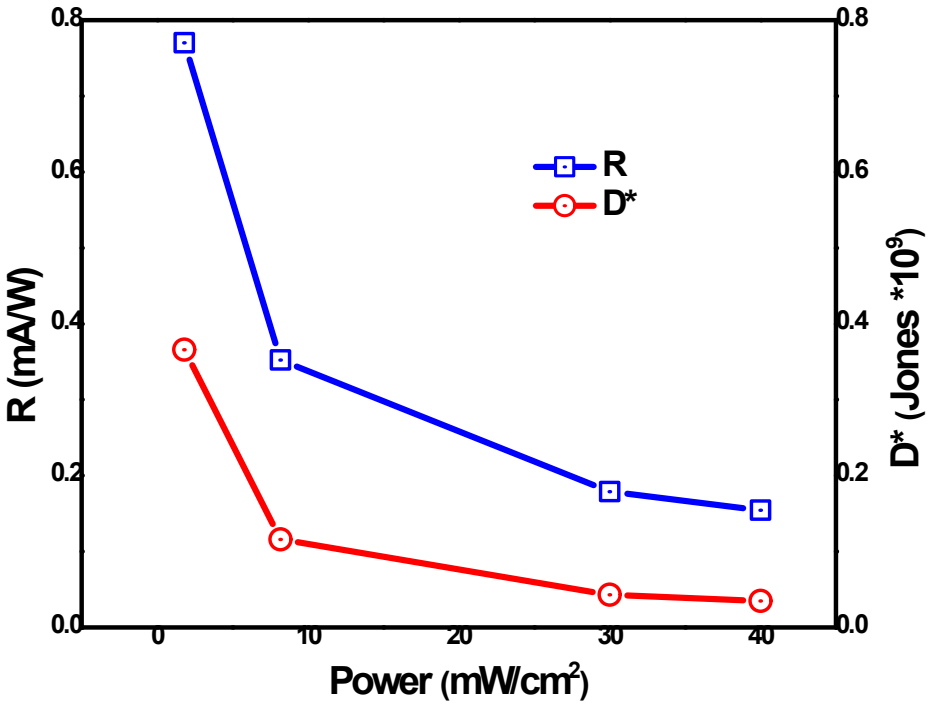

Figure S8. Device responsivity and detectivity as a function of light intensity of 377 nm light.

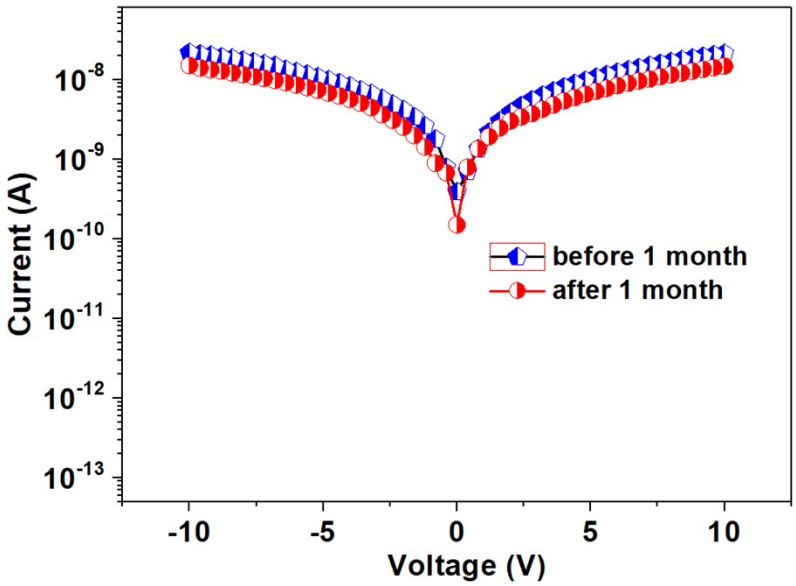

Figure S9. The photostability of **1** verified by the photoconductity properties before and after 1 month under 266 nm illumination.

Table S1. Crystal Data and Structure Refinement for **1**.

Formula	$(C_6H_{12}N_2H_6)$ Cs Pb_2Br_7
Formula weight (g/mol)	1224.88
Temperature (K)	273K
Crystal system	orthorhombic
Space group	$Pca2_1$
a (Å)	8.2772 (5)
b (Å)	8.0905 (4)
c (Å)	35.589 (2)
α (deg)	90
β (deg)	90
γ (deg)	90
Volume (Å^3)	2383.3 (2)
Z	4
D_{calcd} (g/cm3)	33.414
F (000)	2128.0
Radiation	MoKα (λ = 0.71073)
limiting indices	$-10 \le h \le 10$, $-10 \le k \le 10$, $-45 \le l \le 45$
Reflns collected	33423
Independent reflections	5263 [R_{int} = 0.0842, R_{sigma} = 0.0564]
Data/restraints/parameters	5263/19/167
Goodness-of-fit on F^2	0.996
completeness (%)	100
final R indices [$I>2\sigma(I)$]	R_1 = 0.0401, wR_2 = 0.0794
R indices (all data)	R_1 = 0.0847, wR_2 = 0.0965

[a] $R_1 = \sum||F_o| - |F_c||/\sum|F_o|$; $wR_2 = \{\sum[w(F_o^2 - F_c^2)^2]/\sum w[(F_o)^2]^2\}^{1/2}$

Table S2. Perovskite hybrid for photodetection.

Material structure	Device type	Light (nm)/power (mW cm^{-2})	On-off ratio	Charge trap density (cm^{-3})	Dark current (A)	Ref.
$(2meptH_2)CsPb_2Br_7$	Photoconductor	266 (37.5)	1.2×10^3	7.3×10^{10}	1.7×10^{-11}	the present work
$(CH_3NH_3)PbCl_3$	Photoconductor	365 (1000)	1.1×10^3	3.1×10^{10}	4.15×10^{-7}	1
$(CH_3NH_3)PbBr_3$	Photoconductor	520 (1)	30	5.8×10^9	3×10^{-8}	2, 3
$(CH_3NH_3)PbI_3$	Photoconductor	660 (3.9)	10^3	3.6×10^{10}	4×10^{-9}	3, 4
$(PA)_2(MA)_2Pb_3Cl_{10}$	Photoconductor	266 (6500)	2.3×10^3		10^{-8}	5
$(C_4H_9NH_3)_2CsPb_2Br_7$	Photoconductor	365	10^3		1.8×10^{-11}	6
$EA_4Pb_3Br_{10}$	Photoconductor	405	10^3		1.64×10^{-10}	7
$(C_4H_9NH_3)_2PbBr_4$	Photoconductor	470 (0.2)	10^3		10^{-10}	8
$(C_5H_{11}NH_3)_2(MA)Pb_2I_7$	Photoconductor	600 (80)	10^3	5.5×10^{10}	1.1×10^{-10}	9

(1) G. Maculan; A. D. Sheikh; A. L. Abdelhady; M. I. Saidaminov; M. A. Haque; B. Murali; E. Alarousu; O. F. Mohammed; T. Wu; O. M. Bakr,. $CH_3NH_3PbCl_3$ Single Crystals: Inverse Temperature Crystallization and Visible-Blind UV-Photodetector. *J. Phys. Chem. Lett.* **2015**, *6*, 3781-3786.

(2) D. Shi; V. Adinolfi; R. Comin; M. Yuan; E. Alarousu; A. Buin; Y. Chen; S. Hoogland; A. Rothenberger; K. Katsiev; Y. Losovyj; X. Zhang; P. A. Dowben; O. F. Mohammed; E. H. Sargent; O. M. Bakr,. Low trap-state density and long carrier diffusion in organolead trihalide perovskite single crystals. *Science* **2015**, *347*, 519-521.

(3) J. Xin; Q. Wang; J. Li; K. Wang; W. Deng; J. Jin; M. Peng; M. Fang; J. Qu; H. Wang,. Planar visible–near infrared photodetectors based on organic–inorganic hybrid perovskite single crystal bulks. *Journal of Physics D: Applied Physics* **2020**, *53*.

(4) Q. Dong; Y. Fang; Y. Shao; P. Mulligan; J. Qiu; L. Cao; J. Huang,. Electron-hole diffusion lengths >175 mm in solution-grown $CH_3NH_3PbI_3$ single crystals. *Science* **2015**, *347*, 967-969.

(5) Z. Xu; W. Weng; Y. Li; X. Liu; T. Yang; M. Li; X. Huang; J. Luo; Z. Sun,., 3D-to-2D Dimensional Reduction for Exploiting a Multilayered Perovskite Ferroelectric toward Polarized-Light Detection in the Solar-Blind Ultraviolet Region. *Angew. Chem. Int. Ed.* **2020**, *132*, 2-7.

(6) Z. Wu; C. Ji; L. Li; J. Kong; Z. Sun; S. Zhao; S. Wang; M. Hong; J. Luo,. Alloying n-Butylamine into $CsPbBr_3$ To Give a Two-Dimensional Bilayered Perovskite Ferroelectric Material. *Angew. Chem. Int. Ed.* **2018**, *57*, 8140-8143.

(7) S. Wang; X. Liu; L. Li; C. Ji; Z. Sun; Z. Wu; M. Hong; J. Luo,. An Unprecedented Biaxial Trilayered Hybrid Perovskite Ferroelectric with Directionally Tunable Photovoltaic Effects. *J. Am. Chem. Soc.* **2019**, *141*, 7693−7697.

(8) Z. Tan; Y. Wu; H. Hong; J. Yin; J. Zhang; L. Lin; M. Wang; X. Sun; L. Sun; Y. Huang; K. Liu; Z. Liu; H. Peng,. Two-Dimensional $(C_4H_9NH_3)_2PbBr_4$ Perovskite Crystals for High-Performance Photodetector. *J. Am. Chem. Soc.* **2016**, *138*, 16612-16615.

(9) S. Han; P. Wang; J. Zhang; X. Liu; Z. Sun; X. Huang; L. Li; C. Ji; W. Zhang; B. Teng; W. Hu; M. Hong; J. Luo,., Exploring a Polar Two-dimensional Multi-layered Hybrid Perovskite of $(C_5H_{11}NH_3)_2(CH_3NH_3)Pb_2I_7$ for Ultrafast-Responding Photodetection. *Laser Photon. Rev.* **2018**, *12*, 1800060.